# Topography-based Tectonic Evidence for Longitudinal Magma Migration Under the Southern Mid-Atlantic Ridge

**By Simon Detmer, Adam Tjoelker, C. Renee Sparks**
Calvin University
Department of Geology, Geography, and Environment

## Abstract

*Mid-ocean ridge systems are essential for the generation of new crust and are important sources of volcanism, but many aspects of the tectonic forces governing their dynamics remain unresolved. In this study of the Mid-Atlantic Ridge system over latitudes between the equator and 30°S, mapping of ocean floor topography reveals tensional stresses between ridge and transform segments. Orthogonal fracture sets provide evidence of rotation, faulting, and shearing during ridge evolution. Current models of magma genesis suggest the vertical and lateral movement of melt generated by decompression is associated with asthenospheric upwelling and plate divergence. The conceptual model presented in this research evaluates the potential of magma migrating northward in addition to upwelling, extending the traditional two-dimensional model of a triangular melt generation region to a three-dimensional triangular prism. Variations in lithostatic load may slowly drive longitudinal migration of melts northward toward the equa-tor. Shear forces arising from Coriolis effects may act on northward-flowing magmas resulting in increased stress exerted on existing faults to produce the observed geometry of the southern Mid-Atlantic Ridge system.*

**Introduction**

Our understanding of mid-ocean ridge (MOR) systems is coming into clearer focus with increased knowledge of ocean floor topography as well as geophysical insights into subsurface structure and properties. Structural understanding of the fracture and fault orientations represented within the topography of MOR systems may elucidate corresponding stress regimes, providing insight into tectonic forces. After reviewing major MOR systems around the world, we chose to examine interactions between topographical structures and forces affecting magmatic and tectonic movement in the southern Mid-Atlantic Ridge (MAR) system between latitudes 1.5˚S and 30˚S. This region was chosen for the relative simplicity of its tectonic setting. The lower-latitude southern MAR where the South American and African plates diverge from each other is flanked on either side by passive continental margins, reducing the effect of lithospheric slab pull on local ridge system dynamics. It is also distanced from triple junctions where plate movement is more complex. This study area covers a broad range of latitudes, accommodating a series of ridge segments that trend slightly west of north. In comparison, the longitudinal differences are small, primarily consisting of offsets arising from transform faulting. Within the defined study area, the goal of this research is to describe structural patterns in the MAR ocean floor topography that may reveal unidentified stresses. We also explore the possible role of magma movement in generating these tectonic forces.

*Magma Generation*

Magma movement below the mid-ocean ridges begins with the creation of magma through decompression melting and volatile enrichment. The leading mechanism for magma generation is decompression melting, which occurs as hot mantle rock rises into areas of lower pressure. These low-pressure areas are produced by the divergence of lithostatic plates, allowing high-temperature rock to partially melt under reduced pressure as it rises through the mantle.[2] According to a one-dimensional model of upwelling magma below MOR systems, melting originates in the mantle near a depth of 60 km.[1] Based on this estimate, we performed analyses of magma migration at 50 km below sea level, within the melt triangle supported by theory.[2,3,4] Although slab pull from subduction zones at the opposite end of the plate is considered to be the primary driving force for plate movement,[5,6,7] magma generation may also contribute to a positive feedback system of ridge push characterized by diverging tectonic movement. The newly deposited lava at the ridge axis has a lower density than the neighboring crust, providing an area of decompression below the ridge. As the

ridge is pushed up and away from the center of the earth due to its relative buoyancy, gravitational forces pull the areas adjacent to the ridge axis down and further apart. This allows for continued decompression and the upwelling of magma plumes into a triangular region under the MOR system,[8] as shown in Figure 1, where the triangle is extended as a prism under a ridge segment. The second mechanism for magma generation is induced by volatiles such as water and $CO_2$ that produce localized melting deeper within the mantle. Specifically, an increase in water through the hydrothermal alteration of primarily anhydrous silicates results in an increased melt volume resembling the effect of increased temperature.[8,10,11] This melting allows smaller amounts of magma to form below the typical solidus depth and rise into the larger magma regime, influencing asthenospheric mantle convection.[2]

*Figure 1 - A magmatic prism below a mid-ocean ridge segment.*
*A magmatic prism is produced by decompression melting under divergent segments of a MOR system. The lower limit of the magmatic prism represents the solidus bound by pressure and the upper limit represents the solidus bound by temperature.[9] Melt focuses in the central region of the prism moving vertically through buoyancy and laterally as a result of pressure.[3] Lateral movement from higher pressure toward lower pressure is depicted.*

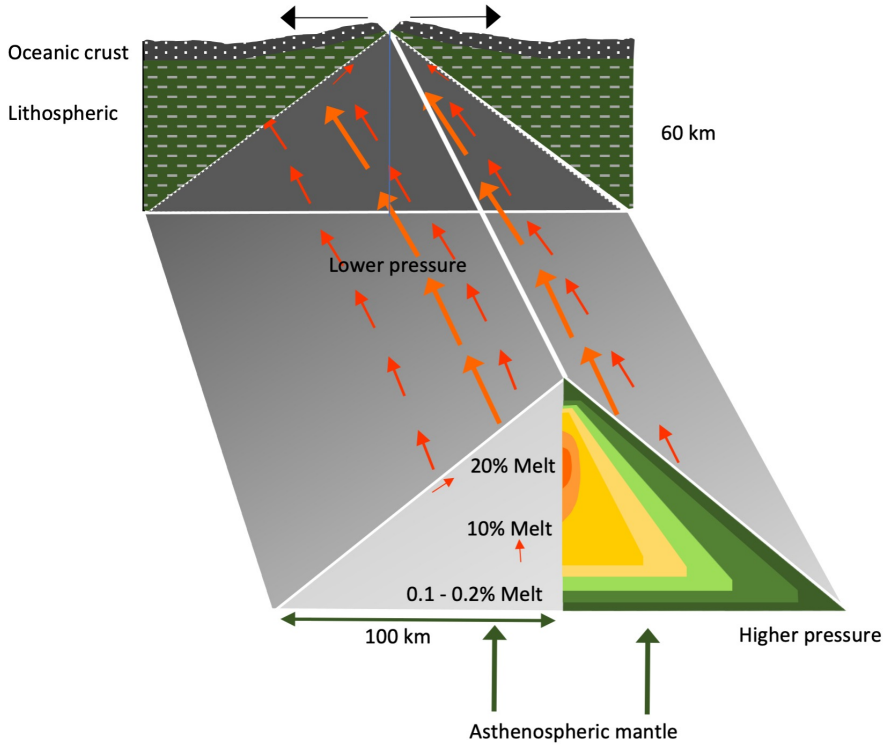


*Magma Migration*

After magma is formed, it tends to migrate upward as a result of buoyancy. Since hot magma is less dense and more buoyant than the residual solid, it will rise into mid-oceanic ridge systems as a component of upper mantle convection.[12] Models such as the Enthalpy Method, which uses conservation of bulk enthalpy to predict melting dynamics in thermodynamic equilibrium, suggest that the rise of magma is accompanied by a decrease in temperature and an increase in melting, porosity, and fluid velocity, such that melt fraction increases from 0% at a depth of 60 km to 20% near the surface.[2,13] These changes decrease magmatic density and drive further vertical movement due to buoyancy. Thus, magma generation below the MOR systems contributes to a net vertical movement towards the crust.

The observed crustal thickness of MOR systems indicates that magma must not only move upward from beneath the ridge axis but also laterally inward. Crustal thickness at MOR systems with spreading rates greater than 15 mm/a is approximately 6-7 km.[3,4] If magma was only generated below the ridge systems, the crustal thickness would be thinner as there is not enough melt to generate a crust with the indicated thickness. Therefore, there must also be a horizontal component to magma migration.[13] The combination of vertical and horizontal magma movement creates a triangular melt regime below the ridge (Figure 1). Magma being produced over 50 km away on either side of the ridge requires a high degree of focusing toward the axis, which is provided by lateral pressure gradients.[2,3,14] The magma directly below the ridge axis rises vertically, not interfering with the lithospheric plates. However, the melt that rises beneath the flanks of the melt triangle may encounter the cooler lithosphere. Since the solid lithosphere is an impermeable layer, pooling of magma may occur at the contact between the asthenosphere and lithosphere, forming a highly porous zone about 100 meters thick by increasing the melt fraction at the top of the asthenosphere.[13] As magma continues to accumulate beneath the solidus, the permeability of the high-porosity layer increases, allowing buoyancy to drive magma along the solidus boundary. The solidus boundary slopes away from the axis due to increasing lithospheric thickness away from the ridge.[13] Buoyancy focuses magma migration toward the region of thinner crust, and, thus, toward the ridge axis.[3] In summary, decompression melting is thought to be the primary magma-producing component under MOR systems. After magma is generated, buoyancy drives its vertical movement upward while the slope of the rigid aesthenosphere-lithosphere boundary focuses magma horizontally within the triangular melt region.

Expanding upon the traditional 2D model where magma flows directly upward or latitudinally in the MAR systems, we propose that longitudinal pressure gradients may also induce an axial component to magma flow. Thus, upwelling occurs in a 3D triangular prism both upward and, to a lesser extent, along the ridge axis either toward or away from the equator (Figure 2C). We proposed this model since Coriolis forces resulting from axial flow along the MAR system may account for the asymmetry noted in our topography of right- and left-lateral transform faults. For comparison, Coriolis forces on a hurricane with a radius of 250 km and

*Figure 2 - Load calculation and pressure gradient.*
*Lithostatic load variations may induce pressure gradients and magma flow in the upper mantle. A demonstrates the assumption of load equilibrium in the crust and mantle whereas B illustrates a more realistic picture of local load variations leading to magma flow in the underlying mantle from regions of high pressure to low pressure. C depicts a possible global variation in lithostatic load due to fluctuations in the gravitational field at the Earth's surface that arise from the ellipticity of the Earth. Shown also are the three layers – water column, mafic ocean crust, and upper mantle – whose weights were incorporated into the calculation of the total load at a depth of 50 km. Loads were calculated with the densities and average thicknesses indicated. Acceleration due to gravity values were determined from latitude based on the empirical equation shown in C sourced from the 1985 NIMA report.[18] The resulting global pressure gradient shows the potential for fluid flow from higher pressure at higher latitudes to lower pressure at lower latitudes given the same average column of weight-bearing material.*

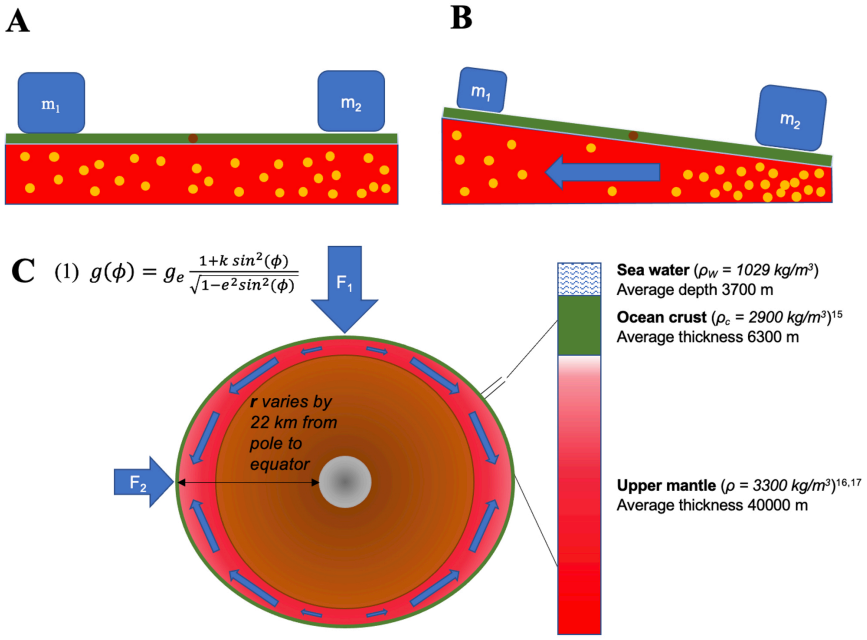


an internal pressure gradient of 0.4 millibars/km produce extremely high wind speeds associated with the pressure gradient force. It should be noted that the viscosity of magma is roughly 105 times that of air and the relevant pressure gradients are 15-fold lower in the asthenosphere, so the fluid velocity induced by Coriolis forces in the asthenosphere will be much lower than hurricane wind speeds.

A reasonable question to ask is whether or not the magma has a low enough viscosity to migrate due to Coriolis forces. Since viscosity is related to temperature and composition, magma movement is more likely in areas with warmer conditions. As the magma rises to shallower depths and cools, the viscosity increases, inhibiting lateral movement. The lateral flow of magma would also be dependent on the permeability and porosity generated by melting within the source rock, as well as the viscosity of magma produced. However, given the long time scales of tectonic migration, the effect of slow but persistent magma movement due to the Coriolis force could be visible in the orientation of fault segments.

Another question our study addresses regards the source of the pressure gradient leading to axial magma migration. One of our hypotheses was that variation in the gravitational field strength due to the equatorial bulge might create a pressure gradient from the poles toward the equator. As Earth spins on its axis, it bulges an additional 22 km at the equator and flattens near the poles, influencing the gravitational values in a predictable manner. The force of gravity experienced at sea level increases with increasing latitude. We explored the possible effect of the global variation in gravitational field strength, as well as more local variations in pressure, by calculating lithostatic load variations at 50 km below sea level. The National Imagery and Mapping Agency published the relationship between latitude (φ) and acceleration due to gravity as an equation as part of the World Geodetic System 1984 (equation 1 in Figure 2C).[18] This relationship calculates the acceleration of gravity at 0° latitude as 9.78032 m/s² (ge) and 9.7932 m/s² at 30°S. The constant used for the ellipsoid shape of the earth (k) is ($1.913185 \times 10^{-3}$) and e is the first eccentricity of the ellipsoid ($6.69438 \times 10^{-3}$).[18] With the acceleration due to gravity determined at each point of interest (g(φ)), the lithostatic load can be calculated as shown in Figure 2C.

(2) $P_{50} = g(\phi)(\rho_w d_w + \rho_c(d_c - d_w) + \rho_m(d_m - d_c))$

Lithostatic load is the pressure occurring at depth in response to the overlying load. It can be expressed as an equation (2) where the density (ρ in kg/m³) is used along with the change in depth (d in m) for three different layers. The sum of these layers represents the lithostatic load as the pressure exerted on the material at 50km depth. In a MOR setting, the layers to evaluate include the water column of the ocean, oceanic crust, and mantle material. Figure 2 illustrates the column with layers as well as the values used to determine the confining pressure associated with the lithostatic load to a depth of 50 km. It should be noted that vertical gravitational variation was not accounted for in this simplified model. If there is melt is present at this depth, the lithostatic load on that melt will produce a higher pressure where the acceleration due to gravity is higher.

## Methods

Gridded bathymetry information was obtained from the General Bathymetric Chart of the Oceans (GEBCO) website in January 2021. The downloaded fields represent an information product based on interpolation through the application of mathematical algorithms using bathymetric data (15 arc-sec resolution). The GEBCO grid is in the public domain and resulting fields can be placed into ArcGIS software for mapping. Boundary coordinates were entered at the following website https://download.gebco.net/, where ESRI-ASCII files were downloaded to cover the Mid-Atlantic Ridge between the equator and 30 degrees south latitude. (Note:

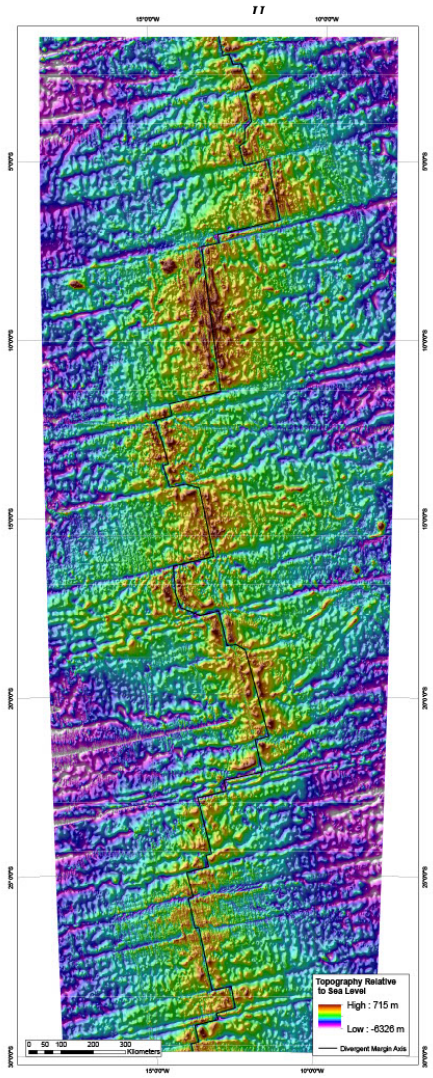


*Figure 3 - Southern Mid-Atlantic Ridge topography.*

*Map of ocean floor topography based on GEBCO products focused on the Mid-Atlantic Ridge system extending from the equator to 30°S. Color raster exhibits red for shallow elevations associated with the ridge system and magenta to white for very deep locations along with hillshading . Structural lineations of ridge and transform segments are outlined in black to highlight the continuum of the divergent plate margin.*

The TID Grid data can be used to distinguish bathymetry data sources. Information about the GEBCO TID Grid can be found at: https://www.gebco.net/about_us/contributing_data/tid_grid.html). ESRI-ASCII files were converted to raster files using spatial analyst tools in ArcGIS to produce a layer representing the ocean-floor topography.

Once the layer was established, a sequential visible spectrum color ramp from white to red was employed to indicate the bathymetry depth. With a color ramp in place, the Hillshade raster tool was used to generate an additional raster file and displayed with 50% transparency above the GEBCO data raster to develop terrain visualization for the data. Maps of the study area were generated from 1.5˚S to 30˚S and between 8˚W and 18˚W with a UTM projection to preserve the geometry of the area mapped. Since the data information spans the boundary of UTM zones 28 and 29 South, a custom UTM zone was made with a central meridian of 13˚W, which was centered on the data set. All other parameters of the custom UTM projection remained the same as the standard UTM southern zones. For an accurate representation of the data from the bathymetry rasters, all rasters must be set to use the projection and coordinate system for the area of interest. In this case, rasters were set to the custom UTM projection. Figure 3 shows the mapped topography of the ocean floor in the study area with connected ridge and transform segments identified.

With the study area represented in a raster map form, the ridge axis and axial valley were identified and delineated. Hillshading and color ramping provided most of the visualization to identify these divergent boundaries. In areas where the ridge system is well-defined with tall ridges to the east and west of a lower rift valley, the ridge line is drawn between the ridges in the center of the lowest part of the valley. When the ridge line reaches a transform fault, the line is drawn along the transform fault until an orthogonal line can then continue along the rift valley. In areas where the rift valley is less defined, but an axis of divergence is apparent due to

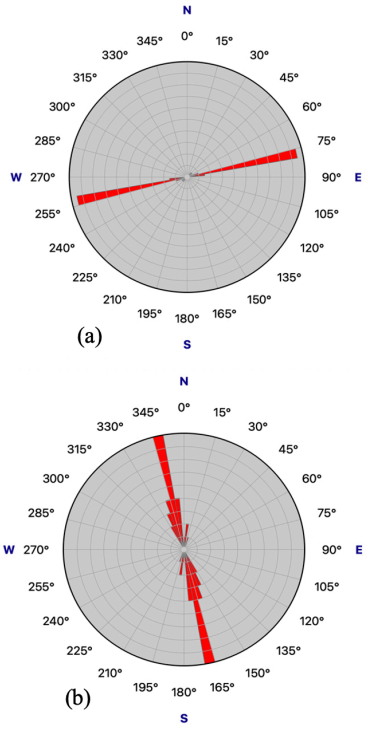


| Azimuth | Number of Transforms |
|---|---|
| 40-45 | 1 |
| 50-55 | 1 |
| 70-75 | 2 |
| 75-80 | 19 |
| 80-85 | 3 |

Table 1

| Azimuth | Number of Ridges |
|---|---|
| 150-155 | 2 |
| 155-160 | 3 |
| 160-165 | 4 |
| 165-170 | 9 |
| 170-175 | 4 |
| 175-180 | 0 |
| 180-185 | 1 |
| 185-190 | 2 |
| 190-195 | 0 |
| 195-200 | 1 |

Table 2

*Figure 4 - Structural azimuths of the southern MAR system.*

*In reference to the Mid-Atlantic Ridge (1.5-30˚), (a) plots the azimuths of 26 of the transforms indicated in Table 1, (b) plots the azimuths of the 26 ridges indicated in Table 2.*

a partial rift valley north and south of a high region in the ridge topography, the line is drawn to connect directly between the apparent lower areas of the rift valley. An example of this is seen in the divergent margin south of the Ascension Fracture Zone.

Forty topographic cross-sections were also used to verify the placement of major faults that define the divergent boundary. In other areas of the divergent margin, occasionally, the lowest part of the rift valley appeared to not conform to a strict path with orthogonal changes in direction and rather appeared to have a diagonal direction containing many transform faults between transform faulting boundaries and the typical orientation of the divergent margin. In these areas, the line was drawn to best conform to the lowest area of the rift valley and may take on an occasional diagonal path that is not orthogonal to the normal faulting direction and not oriented with the typical transform faulting direction. A more detailed analysis, using a higher resolution bathymetry data set than is currently publicly available, could result in subdividing these diagonally drawn sections into a set of multiple transform faulting regions.

*Figure 5 - Conceptual model of tectonic development in the southern MAR system.*

*Conceptual model of tectonic forces leading to the current orientation of the Southern Mid-Atlantic Ridge from 30°S latitude toward the equator. Stage 1 illustrates an idealized N-S trending ridge with tensional stresses producing divergence and orthogonal fracture sets. The larger vector shows a pressure gradient force toward lower latitudes associated with lithostatic load based on gravitational differences, while the smaller vector shows the Coriolis term of force. Stage 1 to Stage 2 illustrates a slight counterclockwise rotation of the system including major fracture sets. During Stage 2, shear stresses from the Coriolis force produce transform movement as shown by smaller right-lateral arrows, off-setting the ridge segments to develop Stage 3 as a segmented ridge. Ridge segments could also experience counterclockwise rotation resulting in some left-lateral, smaller-scale stress accommodation.*

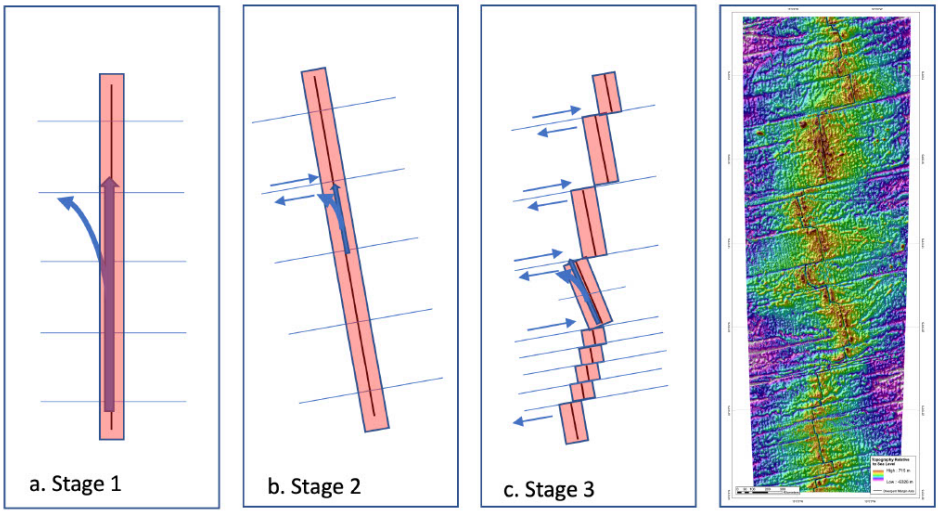


**Results**

Connected ridge and transform segments delineate the divergent plate boundary in the study area as a result of topographic analysis and provide the basis for structural analysis associated with tectonic forces. A total of 26 ridge segments, 26 transform segments, and three oblique connecting fault lines were identified in this study. Identified transform segments found in the study area are plotted in Figure 4. The predominant direction of the major southern transform faulting is between 75˚ and 80˚ (73% of the azimuths). Additional analysis indicates that 69% of the transform faults exhibit a right-lateral, strike-slip movement. Furthermore, of the 19 transforms that extend beyond the ridge zone longitudinally, 16 show right-lateral movement, and 18 have azimuths between 75˚ and 80˚. Analysis of the ridge segments shows an orthogonal relationship to the transform faults with azimuths between 165˚ and 170˚.

Comparable depths at different latitudes exert differential lithostatic loads producing a pressure gradient toward decreasing latitudes for an equivalent depth. The pressure gradient calculated by Equation 2 showed a change in lithostatic load of 2.1 MPa over a distance of 30° latitude, 6.36 millibars per kilometer. A simplified model of magma movement in MOR systems suggests that the difference in gravity may induce an overall flow from higher pressures at higher latitudes to lower pressures in equatorial regions. However, to understand the significance of these calculated variables, a linear flow velocity was calculated using constants specified in earlier studies.

(3) $$u = \frac{k_0 \varphi^2}{\mu L} \Delta p$$

The predicted linear flow velocity of the magma moving northward is calculated using a rearrangement of Darcy's law and the standard equation for flow velocity (equation 3). This calculation assumes a controlled environment where only a few variables are considered. In this calculation, u is the flow velocity in m/s, μ is the dynamic viscosity (Pa-s), ϕ is the porosity (p=0.02)[3], L is the length of the ridge (3.33 x $10^6$m for MAR 1.5-30˚ South), Δp is the pressure difference between the two depths, and $k_0$ is the permeability $10^{-9}m^2$.[3,13] The calculated velocity of magma is $2.5x10^{-3}$ cm/yr, which is three orders of magnitude smaller than MOR systems' spreading rates.

(4) $$f = 2\Omega \, sin \, sin \, (\phi)$$

(5) $$Ro = \frac{U}{Lf}$$

(6) $$\frac{\Delta P}{L} = \frac{u\mu}{k_0 \varphi^2}$$

Using the Rossby number (Equation 5) to compare the importance of length vs. the calculated velocity of the magma flow through the system, and Darcy's law (Equation 6) to compute the fluid velocity induced in a viscous liquid by pressure gradients, we find that the pressure differential required to create magma movement in the decompression melting zone comparable to upwelling is on the order of 10 MPa/km. The calculated velocity of magma due to variation in the gravitational field strength at different latitudes is $2.5x10^{-3}$ cm/yr, which is three orders of magnitude smaller than MOR systems' spreading rates, but may contribute long-term over

many millennia if it is not canceled out by other forces and is constant long term. While this exceeds the pressure gradients attributable to global variation in the gravitational field strength on the Earth's surface, it does not rule out local variations in lithostatic load which may lead to pressure gradients of the required strength to induce axial magma migration subject to Coriolis forces.

**Interpretation and Conclusions**

*Model of Structural Deformation*

Structural data collected from the GEBCO information supports the tensional stresses expected for a divergent margin with orthogonal fracture sets. Normal faults and tension fractures are the most common structural elements of MOR systems.[19] With an upwelling asthenosphere, the oceanic crust would experience tensional stress producing fracture sets at 90 degrees to one another. The starting orientation of the fracture set would be related to the stress field experienced nearly 80 Ma ago during the westward migration of the ridge system.[20] This would produce a stress field with $\sigma_1$ related to upwelling, $\sigma_3$ associated with the westward drift providing the tension, and $\sigma_2$ neutral, which would result in N-S and E-W conjugate sets of fractures.[21] Our conceptual model, shown in Figure 5, is initiated with a set of orthogonal fractures oriented with ridge segments striking N-S.

Although this study uses GIS to identify a path for these major faults, the path typically represents a set of parallel fractures visible in areas where the bathymetry is higher resolution. These fracture sets have been recognized in basalt flows exposed in Iceland with fault swarm areas of 5-10 km width and 40-80 km length[19] and are similar in size when considered within much of the MAR within the study area. It is likely that the fracture sets start with a vertical opening but then develop into normal faults parallel to the ridge axis. Examples of this can be seen in Iceland, where nucleation of normal faults occurs on inclined fractures shifting to dip-slip movement at a depth of 0.5 km.[19] Brittle deformation associated with the ridge segments would be accommodated by normal faulting facilitating decompression, upwelling asthenosphere, and magma generation within the prism shown in Figure 1.

Though there may or may not be additional melt at depth, this study focuses on the decompression melt prism directly under the ridge system. As with the regional flow of air or water, these materials are subject to the Coriolis parameter of force induced by shearing associated with Earth rotation. This shearing causes a deflection to the left in the southern hemisphere, as shown by the smaller arrow in Stage 1 of Figure 5. At these transform faults, the Coriolis force could lead to the counterclockwise rotation we see evident in the southern hemisphere along the MAR system.[22] If the initial fracture orientation was N-S, rotation due to the Coriolis parameter of force is modeled to be approximately 10 degrees in a counterclockwise direction. Should the entire area rotate equally, the ridge will remain linear.

During Stage 2 of the conceptual model, the rotated transform faults are exposed to a greater shearing and begin to offset the ridge segments. If magma continues to travel to the north along the pressure gradient, it gets deflected to the left and shears the juncture between the ridge and transform, pulling the southern ridge segment to the west and resulting in an overall right-lateral transform fault movement. Data collected in this study shows that 69% of the transform segments exhibit this relative movement offsetting ridge segments with right-lateral transform faulting, meaning that the remaining transforms have left-lateral movement. In these cases, the left lateral movement could be related to brittle deformation above the magma prism as it rotates in a counterclockwise direction. As a result, we can conclude that between 1.5˚ and 30˚ south, ridge orientations and relationships are primarily controlled by the shearing at the ridge to transform junctures.

*Magma migration interpretation*

Considering the combined net movement of magma migration, further analysis of crustal thickness, faulting, and gravitational variance indicates that the Coriolis parameter (f in equation 4) may play a role in MOR system formation and evolution in conjunction with the aged rotation rate of the earth ($\Omega = 7.29 \times 10^{-5}$ Rad/s). The Coriolis effect is indicated by the Rossby number (Ro in equation 5), which is the ratio between the force of inertia and the Coriolis parameter induced over a specified distance.[23] The dynamic fluid mechanics of magma movement within the Earth's asthenosphere as expressed by the Coriolis parameter causes large-scale circulation of matter (e.g. air and water) to rotate clockwise in the northern hemisphere and counterclockwise in the southern hemisphere. If the prismatic magma source regions are affected by the Coriolis parameter, then a westward migration would be present at the equator as the clockwise and counterclockwise rotations come together. Recent research regarding subduction zones indicates a westward drift along the margins supporting large-scale motion that could be connected to the Coriolis parameter of force.[22,23,24] Geochemical assessment of magma movement in a MOR system supports this idea.[25] Additionally, a study surveying nine transverses over MOR systems reveals that heat flow asymmetry favors the westward side in the southern hemisphere.[26] This lateral movement would be governed by pressure differential, causing magma to migrate from higher latitudes to lower latitudes. Magma also has the potential to pool at depth, producing additional magmatic movement such as the northerly flow of magma under the ridge system between 7°30'S to 11°30'S of the Ascension Fracture Zone and the Bode Verde Fracture Zone indicated by isotopic studies.[27] Magma pooling and subsequent migration could introduce additional stresses and magma movements that may be affected by the Coriolis force.[20,28,29] Given that magmatic mass under the MAR may move toward the equator through a variety of mechanisms, stress can build along existing fault planes where ridge segments meet transform faults.

*Conclusions*

Topological analysis of faulting along the Mid-Atlantic Ridge provides evidence for rotation and westward drift, suggesting the influence of forces and flows that generate shear stress as important contributors to tectonic plate movement. The model presented suggests an additional latitudinal component of magma migration along mid-oceanic ridge systems. Based on the calculated gravitational forces and seafloor depths along the Mid-Atlantic Ridge system 0-30˚ south and the predicted pressure loads at a 50 km depth, a 2.1 MPa differential along the ridge system is estimated. If the viscosity of the melt fraction is low enough and magma can flow, the expected flow direction under the

ridge would be toward lower latitudes. With flow, the magma migration would be subjected to shearing, possibly associated with the Coriolis parameter of force or westward drift, to induce stress on existing faults. This stress would manifest as right-lateral, strike-slip movement on existing transform faults, producing a model with similar geometry to the Southern Mid-Atlantic Ridge. Further research regarding magma movement and mega-scale tectonic faulting is required to understand the relationship more clearly between magma movement and mid-oceanic ridge development. Additional studies analyzing the relationship between fluid dynamics, rock porosity, and permeability, or comparing faulting stress dynamics along tectonic boundaries would provide more insight into the dynamics of these ridge systems.

*Acknowledgments*

This research was funded through the Michigan Space Grant Consortium no. NNX-15AJ20H with support from the National Aeronautics and Space Administration.

**References**

[1]Ribe, N. M. (1985) "The generation and composition of partial melts in the earth's mantle." Earth and Planetary Letters 73.2-4. Pg. 361-376.

[2]Plank, T. and Langmuir, C. H. (1992) "Effects of the melting regime on the composition of the oceanic crust." Journal of Geophysical Research 97.B13. Pg 19,749-19,770.

[3]Katz, R.F. (2008) "Magma dynamics with the Enthalpy Method: benchmark solutions and magmatic focusing and mid-ocean ridges." Journal of Petrology 49.12. Pg 2099-2121.

[4]Brown, J.W., and White, R.S. (1994) "Variation with spreading rate of oceanic crustal thickness and geochemistry." Earth and Planetary Science Letters 121.3-4 Pg 435-449.

[5]Forsyth, D., and Uyeda, S. (1975) "On the relative importance of the driving forces of plate motion." Geophysical Journal International 43.1. Pg 163–200.

[6]Lithgow-Bertelloni, C., and Richards, M.A. (1998) "The dynamics of Cenozoic and Mesozoic plate motions." Reviews of Geophysics 36.1. Pg 27–78.

[7]Schellart, W.P. (2004) "Quantifying the net slab pull force as a driving mechanism for plate tectonics." Geophysical Research Letters 31.7. Pg 1-5.

[8]Kelley, K.A. (2014) "Inside Earth runs hot and cold." Science 344.6179. Pg 51-52.

[9]Sim, S.J., Spiegelmam, M., Stegman, D.R., and Wilson C. (2020) "The influence of spreading rate and permeability on melt focusing beneath mid-ocean ridges." Physics of the Earth and Planetary Interiors 304. Pg 106486.

[10]Dasgupta, R., and Hirschmann, M.M. (2010) "The deep carbon cycle and melting in Earth's Interior" Earth and Planetary Letters 298.1-2. Pg 1-13.

[11]Asimow, P.D., and Langmuir, C.H. (2003) "The importance of water to oceanic mantle melting regimes." Nature 421. Pg 815-820.

[12]Lin, J., and Parmentier, E. M. (1989) "Mechanisms of lithospheric extension at mid-ocean ridges." Geophysical Journal 96.1. Pg 1-22.

[13]Sparks, D.W., and Parmentier, E.M. (1991) "Melt extraction from the mantle beneath spreading centers." Earth and Planetary Letters 105. Pg 368-377.

[14]The MELT Seismic Team. (1998) "Imaging the deep seismic structure beneath a mid-ocean ridge: The MELT Experiment." Science 280.5367. Pg 1215-1218.

[15]Carlson, R. L., and Herrick, C.N. (1990) "Densities and porosities in the oceanic crust and their variations with depth and age." Journal of Geophysical Research 95.B6. Pg 9153-9170.

[16]Simon, N.S.C., Neumann, E.-R., Bonadiman, C., Coltorti, M. Delpech, G., Grégoire, M., and Widom, E. (2008) "Ultra-refractory domains in the oceanic mantle lithosphere sampled as mantle xenoliths at ocean islands." Journal of Petrology 49.6. Pg 1223-1251.

[17]Afonso, J.C., Ranalli, G., Fernández, M. (2007) "Density structure and buoyancy of the oceanic lithosphere revisited." Geophysical Research Letters 34.10. Pg 1-5.

[18]Office of Geomatics. (2014) "National Geospatial-Intelligence Agency (NGA) Standardization Document: Department of Defense World Geodetic System 1984 – It's Definition and Relationships with Local Geodetic Systems." Office of Geomatics National Geospatial-Intelligence Agency, Version 1.0.0.

[19]Gudmundsson, A. (1992) "Formation and growth of normal faults at the divergent plate boundary in Iceland." Terra Nova 4.4. Pg 430-527.

[20]O'Connor, J.M., and le Roex, A.P. (1992) "South Atlantic hot spot-plume systems: 1. Distribution of volcanism in time and space." Earth and Planetary Science Letters 113.3. Pg 343-364.

[21]Wise, DU., Funiciello, R., Parott, M, and Salvini, F. (1985) "Topographic lineament swarms: Clues to their origin from domain analysis of Italy." Geological Society of American Bulletin 96.7 Pg 952-967.

[22]Howell, B.F.Jr. (1970) "Coriolis force and the new global tectonics." Journal of Geophysical Research 75.14. Pg 2769-2772.

[23]Levin, B.W., Rodkin, M.V., and Sasorova, E.V. (2017) "Effect of the Earth's rotation on subduction processes." Doklady Earth Sciences 476.3. Pg 343-346.

[24]Carcaterra, A., and Doglioni, C. (2018) "The westward drift of the lithosphere: A tidal rachet?" Geoscience Frontiers 9. Pg 403-414.

[25]Langmuir, C.H., Bender, J.F., Batiza, R. (1986) "Petrological and Tectonic Segmetation of the East Pacific Rise, 5°30'-14°30' N." Nature 322. Pg 422-429.

[26]Khutorskoi, M.D., Teveleva, E.A. (2020) "Nature of heat flow asymmetry on the mid-oceanic ridges of the world ocean." Marine Geology 60.1. Pg 125-137.

[27]Paulic, H., Munker, C., and Schuth, S. (2010) "The influence of small-scale mantle heterogeneities on Mid-Ocean Ridge volcanism: Evidence from the southern Mid-Atlantic Ridge (7°30'S to 11°30'S) and Ascension Island." Earth and Planetary Science Letters 296.3-4. Pg 299-310.

[28]Evangelidis, C.P., Minshull, T.A., and Henstock T.J. (2004) "Three-dimensional crustal structure of Ascension Island from active source seismic tomography." Geophysical Journal International 159.1. Pg 311-325.

[29]Chamberlain, K.J., Barclay, J., Preece, K., Brown, R.J., Davidson, J.P., and EIMF. (2016) "Origin and evolution of silicic magmas at ocean islands: Perspectives from a zoned fall deposit on Ascension Island, South Atlantic." Journal of Volcanology and Geothermal Research 327. Pg 349-360.